AIP | The Journal of Chemical Physics

Donor–acceptor interchange tunneling in HDO–DOH and the higher energy HDO–HOD isotopomer

E. N. Karyakin, G. T. Fraser, F. J. Lovas, R. D. Suenram, and M. Fujitake

Citation: The Journal of Chemical Physics **102**, 1114 (1995); doi: 10.1063/1.469169
View online: http://dx.doi.org/10.1063/1.469169
View Table of Contents: http://scitation.aip.org/content/aip/journal/jcp/102/3?ver=pdfcov
Published by the AIP Publishing

Articles you may be interested in

Modulating emission from acceptor in donor-acceptor diblock copolymers by plasmon resonance energy transfer
J. Appl. Phys. **110**, 114319 (2011); 10.1063/1.3665722

Intramolecular and intermolecular energy transfers in donor-acceptor linear porphyrin arrays
J. Chem. Phys. **125**, 074902 (2006); 10.1063/1.2333509

Diffusion modulated donor–acceptor energy transfer in a disordered system
J. Chem. Phys. **72**, 3528 (1980); 10.1063/1.439615

Determination of the binding energies of shallow acceptors from photoluminescence excitation spectra for donor-acceptor pairs in ZnTe
J. Appl. Phys. **50**, 4958 (1979); 10.1063/1.325571

Shallow acceptor binding energy and lifetime of donor-acceptor pairs in gallium arsenide
J. Appl. Phys. **47**, 3219 (1976); 10.1063/1.323118

Reuse of AIP Publishing content is subject to the terms: https://publishing.aip.org/authors/rights-and-permissions. Downloaded to IP: 144.82.108.120 On: Mon, 05 Sep 2016 11:26:41

Donor–acceptor interchange tunneling in HDO–DOH and the higher energy HDO–HOD isotopomer

E. N. Karyakin
Molecular Spectroscopy Laboratory, Applied Physics Institute, Nizhnii Novgorod, Russia

G. T. Fraser, F. J. Lovas, and R. D. Suenram
Molecular Physics Division, National Institute of Standards and Technology, Gaithersburg, Maryland 20899

M. Fujitake
Department of Physics, Faculty of Science, Kanazawa University, Kakuma, Kanazawa, 920-11 Japan

(Received 6 July 1994; accepted 12 October 1994)

The microwave and submillimeter spectra of the a-type $K=0\leftarrow 0$ and $K=1\leftarrow 1$, c-type $K=1\leftarrow 0$, and isotopically allowed b-type $K=1\leftarrow 0$ bands of the O–D bonded HDO–DOH water dimer isotopomer and the higher energy O–H bonded HDO–HOD isotopomer have been measured using molecular-beam electric resonance optothermal and pulsed-nozzle Fourier-transform microwave spectrometers. The present results obtained in He and He/Ne seeded molecular beams give the first evidence for the presence of the higher energy O–H bonded mixed protonated-deuterated water dimers. These species were not reported previously in studies using seeded Ar molecular beams. The donor–acceptor interchange tunneling splittings are found to be 1322.1019(43) and 5004.059(20) MHz for the HDO–DOH and the metastable HDO–HOD dimers, respectively. For both isotopomers, the donor-accepter interchange tunneling-state selections rules for the b- and c-type bands are consistent with tunneling pathways corresponding to geared partial internal rotation of the two subunits in double-minima potentials. The larger tunneling splitting in HDO–HOD is primarily the consequence of the smaller effective reduced mass for tunneling in this system compared to that in HDO–DOH. The presence of both b- and c-type $K=1\leftarrow 0$ bands allows the direct measurement of the largest tunneling splitting, that associated with the internal rotation about the O–H–O or O–D–O bond of the nonbonded proton/deuteron on the proton donating unit. For the $K=0$ state of HDO–DOH this splitting is 214 208.38(23) MHz, while for the $K=0$ state of HDO–HOD it is 117 440.97(17) MHz. A strong b-type Coriolis interaction is observed between the upper $K=0$ and lower $K=1$ states in HDO–DOH, similar to that observed previously in $(H_2O)_2$. © *1995 American Institute of Physics.*

INTRODUCTION

The high-resolution microwave, far-infrared, and infrared spectra[1–27] of the water dimer have been extensively studied for the last 20 years. Such an effort has been required to unravel the complex multidimensional tunneling dynamics displayed in this system which allows each of the hydrogens to participate in the hydrogen bonding. These tunneling dynamics lead to multiple splitting of the rigid-rotor energy levels. For instance, in the totally protonated or totally deuterated water dimer, proton/deuteron tunneling splits each C_s-symmetry rigid-molecule rotational state into six tunneling components.[3]

The largest tunneling splitting in $(H_2O)_2$ or $(D_2O)_2$ arises from a motion which interchanges the two protons/deuterons on the proton acceptor unit along a tunneling pathway which is thought to be analogous to the amine inversion pathway in methyl amine.[7,13] The next most important tunneling process is the donor-acceptor interchange motion or $(HF)_2$-like tunneling motion which leads to a change of bonding roles of the two moieties in the complex. Both geared and antigeared tunneling pathways have been considered for this motion.[13] Another tunneling process interchanges the two protons/deuterons on the proton donating unit through a bifurcated doubly hydrogen-bonded transition state.[13] In many instances several distinct tunneling pathways are possible to achieve the same final result, giving interference contributions to the tunneling splittings.[13,24]

Despite these dynamical complexities, precise structural data from rotational constant and dipole moment measurements have allowed the water dimer to serve as a test system[28] for the development of *ab initio* electron structure methods. More recent efforts[13,25,29] have shifted to comparing experimental tunneling barriers and pathways with theory. In addition to guiding the development of *ab initio* methods, the spectroscopic measurements furnish data to test and refine proposed pair potentials.[30] An accurate pair potential, when properly supplemented by three-body and higher-order interactions, should be valid over the range of interactions found in the dimer through the liquid and the solid.

The comparison between theory and experiment is limited by the difficulty of relating the experimental tunneling splittings to barrier heights and tunneling pathways which can be calculated theoretically. Although a number of tunneling splittings have been measured, our lack of knowledge of the precise reduced mass for the motion, the shape of the tunneling potential, and the coupling between different tunneling modes, limit our abilities to estimate tunneling barriers. Deuterium isotopic studies, by allowing the tuning of the reduced mass for the tunneling motion, or the elimination of possible tunneling pathways in some instances, can furnish

Reuse of AIP Publishing content is subject to the terms: https://publishing.aip.org/authors/rights-and-permissions. Downloaded to IP: 144.82.108.120 On: Mon, 05 Sep 2016 12:25:12

 0021-9606/95/102(3)/1114/8/$6.00 © 1995 American Institute of Physics

additional information about the tunneling processes. Moreover, deuterium isotopic studies can lead to a partial quenching of the tunneling motions and a reduction of the zero-point motion from that found in the protonated species, thus furnishing a better estimate of the equilibrium properties of the system.

We have recently undertaken a systematic study of the microwave and submillimeter rotational-tunneling spectra of the mixed protonated-deuterated water dimers. The isotopic studies undertaken in seeded He and He/Ne molecular beams reveal the presence of the higher-energy O–H hydrogen bonded mixed H/D species. Previous studies undertaken in seeded Ar beams presumably did not significantly populate these isotopomers. When one considers these isotopomers, there are eleven possible H/D isotopomers present in the molecular beam. Since each of these species gives rise to a complex tunneling-rotational spectrum, radio-frequency microwave or radio-frequency submillimeter double-resonance spectroscopy was used to assign the spectrum. In the present paper we report on two of these isotopomers, HDO–HOD and HDO–DOH, which, if the assumption is made that monomer bonds can not be broken, are the only two isotopomers which belong to the HOD dimer potential energy surface. Several rotational transitions for HDO–DOH were cited previously in a footnote of a report on the O_3–H_2O complex.[31]

The rotational-tunneling spectra of HDO–HOD and HDO–DOH are qualitatively similar.[13] Each rigid-rotor energy level for the two isotopomers is split into four tunneling components. From previous results on $(H_2O)_2$ and $(D_2O)_2$ we anticipate that the largest tunneling splitting arises from a motion which interchanges the H and D on the proton-acceptor unit. This splitting is expected to be on the order of 100 GHz. The second largest tunneling splitting arises from the interchange of the donor and acceptor roles of the two units. This splitting is expected to be intermediate between the 586.058 (7) (Refs. 7, 10, 15, and 32) and 11 277.19 (15) MHz (Refs. 14 and 32) values found for $(D_2O)_2$ and $(H_2O)_2$ dimer, respectively.

Figure 1 shows a qualitative energy-level diagram for the $K=0$ and 1 states of HDO–HOD or HDO–DOH. Also shown in Fig. 1 are the selection rules and the statistical weights. We note that in the case of $(H_2O)_2$ and $(D_2O)_2$, no *b*-type transitions are possible due to the plane of symmetry in the complex. The absence of *b*-type transitions prevents the direct measurement of the largest tunneling splitting, that associated with the interchange of the two protons or deuterons on the proton acceptor unit. Thus, for those isotopomers with a plane of symmetry this splitting has to be inferred from the model Hamiltonian used to fit the spectrum.

The present results lead to a complete characterization of the $K=0$ and $K=1$ energy levels for the HDO–DOH and HDO–HOD isotopomers. The donor-acceptor tunneling splitting is found to be 1322.1019 (43) MHz for the HDO–DOH isotopomer and 5004.059 (20) MHz for the metastable HDO–HOD isotopomer. The larger tunneling splitting in HDO–HOD is mainly the consequence of the much smaller reduced mass for tunneling in this system compared to that in HDO–DOH. The energy level splittings associated with

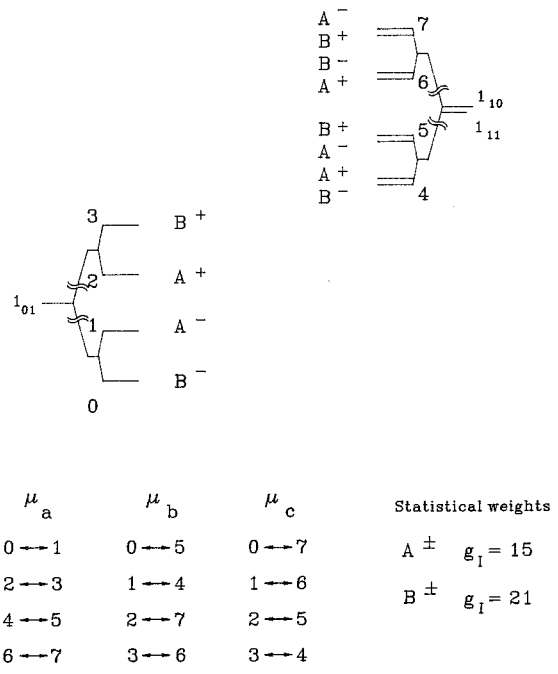

FIG. 1. Energy-level diagram for the $J=1$ rotational-tunneling states of HDO–DOH and HDO–HOD. The tunneling states are labeled $V=0-7$. The states are classified using a molecular symmetry group isomorphic to C_{2v} and C_{2h} as given by Ref. 13. The nuclear-spin statistical weights, g_I, and selection rules, $V' \leftrightarrow V''$, for *a*-, *b*-, and *c*-type transitions are also given.

the methyl-amine-type tunneling and the $K=1 \leftrightarrow 0$ separation for HDO–HOD are similar to those observed for HDO–DOD,[24,33] indicating that the proton-donating H/D plays a minimal role in the methyl-amine tunneling and $K=1 \leftrightarrow 0$ splittings observed in the water dimer system.

EXPERIMENT

The molecular-beam electric resonance optothermal spectrometer used in the present investigation has been described previously.[14,34,35] Briefly, a molecular beam of water dimer is formed by a 300 kPa (3 atm) expansion of He saturated with partially deuterated water vapor through a 40 μm diameter nozzle. The resulting rotational temperature is estimated from previous studies to be between 5 and 10 K. Approximately 2.5 cm from the nozzle the molecular beam is defined by a 1 mm diameter skimmer after which it enters a 56 cm long electrostatic field of quadrupolar symmetry. The quadrupole field focuses or collects molecules in rotational-tunneling states whose energies increase with electric field strength (i.e., have a positive Stark coefficient) onto a 1.7 K liquid-He-cooled Si bolometer detector[36] located along the molecular beam axis approximately 90 cm from the nozzle. Molecules in rotational-tunnelings states whose energies decrease with electric field strength are deflected out of the molecular beam.

Between the nozzle and skimmer the molecular beam is crossed by microwave/submillimeter radiation coming from a cutoff section of *K*-band waveguide. Commercially available microwave synthesizers are used for frequencies less

Reuse of AIP Publishing content is subject to the terms: https://publishing.aip.org/authors/rights-and-permissions. Downloaded to IP: 144.82.108.120 On: Mon, 05 Sep 2016 21:20:40

than 21 GHz and between 54 and 118 GHz and a laboratory submillimeter synthesizer[37] is used for frequencies greater than 150 GHz. Frequencies between 21 and 41 GHz are obtained by doubling and amplifying the output of the lower frequency synthesizer. The microwave or submillimeter radiation is amplitude or frequency modulated at ≈400 Hz for phase-sensitive detection. A transition is observed as a change in beam flux at the bolometer. This change occurs when the molecules in the upper and lower state of the transition have different focusing characteristics in the quadrupole field.

A radio-frequency antenna is also placed between the nozzle and skimmer for double-resonance studies.[38] Radio-frequency double-resonance measurements are made by monitoring the signal strength of a microwave line while tuning the radio-frequency source.

In studying the isotopic water dimer system, survey spectra were recorded over a broad frequency region, covering approximately 150 to 400 GHz. A sample spectral window is shown in Fig. 2. Since most of the transitions in this region are expected to be of the $K=1\leftarrow 0$ type, radio-frequency submillimeter double resonance was attempted on the stronger lines to look for transitions across the $K=1$ asymmetry-tunneling splitting. Such a double-resonance spectrum is shown in Fig. 2. The fact that the donor–acceptor tunneling splitting for the two isotopomers of $(HOD)_2$ differ by factors of 3–5 and that the tunneling splitting vanishes for all the other species except for the well characterized totally protonated or deuterated dimer allows radio-frequency double resonance to be used to make species identification and J and K assignments. In the absence of Coriolis perturbations, the $K=1$ asymmetry-tunneling transitions have frequencies,

$$\nu \cong \left| \nu_t \pm \frac{(B-C)}{2} J(J+1) \right|, \tag{1}$$

where ν_t is the hypothetical $J=0$ tunneling splitting between states $V=7$ and 6 or between states $V=4$ and 5 in Fig. 1.

Several measurements below 25 GHz were made using a pulsed-nozzle Fourier-transform microwave spectrometer of the Balle–Flygare type.[39] The details of the NIST instrument have been described previously.[40–42] Measurements were made both with the nozzle mounted coaxial[43] with the cavity and perpendicular[39] to the cavity. The use of a He/Ne carrier gas allows the observation of the metastable O–H bonded dimers, which were missed in previous studies using Ar as a carrier gas. It has been noted previously[35,44] that Ar gives a significantly colder ''isomer'' temperature than either He or Ne.

RESULTS

The observed transitions for HDO–HOD and HDO–DOH are listed in Table I. For both isotopomers *a*-, *b*-, and *c*-type transitions are observed, with the *b*-type transitions being allowed by the absence of a plane of symmetry for the complex. These observations are in accord with our measurements on HDO–DOD where *a*-, *b*-, and *c*-type transitions were observed. In both $(H_2O)_2$ and $(D_2O)_2$ only *a*- and

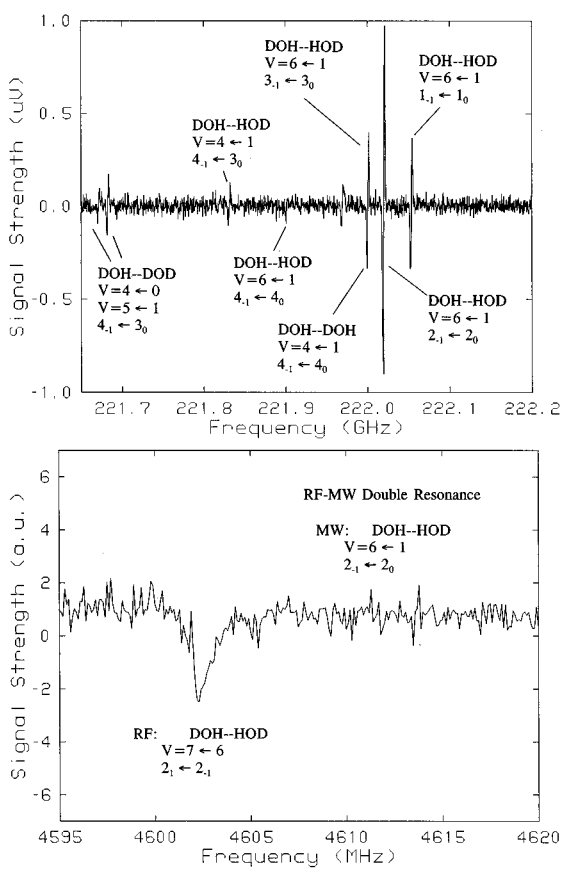

FIG. 2. The upper frame presents a spectral window near 222 GHz for partially deuterated water dimer showing the $V=6\leftarrow 1$ Q branch of HDO–HOD. Transitions are also observed for HDO–DOD and HDO–DOH in this region. The $J=4\leftarrow 3$, $K=-1\leftarrow 0$ transition for HDO–DOD is split into a doublet from a tunneling motion which interchanges the two deuterium nuclei on the proton-donating unit. Nuclear-spin statistical weight considerations give the observed 1:2 intensity ratio. The spectrum was recorded in 10 min. The lower frame shows a radio-frequency-microwave double-resonance spectrum for HDO–HOD. The microwave oscillator is set to the frequency of the $J=2\leftarrow 2$, $K=-1\leftarrow 0$, $V=6\leftarrow 1$ transition shown above at 222 019.63 MHz while the radio-frequency oscillator is tuned through the $J=2\leftarrow 2$, $K=1\leftarrow -1$, $V=7\leftarrow 6$ transition at 4602.52 MHz. The spectrum was acquired in approximately 1.5 min.

c-type transitions are observed. The transitions are labeled by J, K, and V where $V=0-7$ are associated with tunneling states 0–7 in Fig. 1. In Table I we use $K=0$, 1, and -1 to denote the $J_{0,J}$, $J_{1,J-1}$, and $J_{1,J}$ levels, respectively, where the subscripts on J give the limiting prolate and oblate quantum-number labels for an asymmetric rotor state. The observed transitions are least-squares fit to the frequencies calculated from the energy-level expression,

$$E(J,K,V)=E_V\bar{B}_V[J(J+1)-K^2]-D_V[J(J+1)-K^2]^2 + \frac{(B-C)_V}{4} KJ(J+1), \tag{2}$$

valid for the $K=0,\_-1$, and 1 labels of Table I. Here, E_V is the energy origin, $B_V=(B+C)_V/2$, D_V is a centrifugal distortion constant, and B and C are rotational constants characteristic of state V. For HDO–DOH the $V=2$ and 3 levels

Reuse of AIP Publishing content is subject to the terms: https://publishing.aip.org/authors/rights-and-permissions. Downloaded to IP: 144.82.108.120 On: Mon, 05 Sep 2016 21:20:40

TABLE I. Observed transition frequencies for HDO–DOH and HDO–HOD (in MHz). The measurement uncertainties on the transition frequencies are estimated to be ±0.25 MHz, except for the 13 120.121, 10 477.401, 24 915.533, and 22 277.273 MHz lines from Ref. 31 and the 17 597.535 MHz line where the uncertainties are ±0.004 MHz and the 16 303.261 line where the uncertainty is ±0.01 MHz.

J'	V'[a]	K'[b]	J''	V''	K''	HDO–DOH	HDO–HOD
1	1	0	0	0	0	13 120.121	16 303.261
2	1	0	1	0	0	24 915.533	27 600.15
3	1	0	2	0	0	36 707.24	38 893.53
5	1	0	4	0	0	60 275.48	61 466.31
4	3	0	4	0	0	214 086.88	
3	5	−1	4	0	0	175 181.56	
1	5	1	1	0	0	222 900.84	185 724.06
2	5	1	2	0	0	223 296.90	
3	5	1	3	0	0	223 844.84	
4	5	1	4	0	0	224 510.84	186 045.28
5	5	1	5	0	0	225 269.64	186 223.58
1	5	−1	0	0	0	234 435.78	196 957.94
2	5	−1	1	0	0	246 126.86	208 196.08
3	5	−1	2	0	0	257 762.33	
4	5	−1	3	0	0	269 340.50	230 573.16
5	5	−1	4	0	0	280 861.66	241 711.01
6	5	−1	5	0	0		252 813.91
5	7	1	6	0	0	273 419.96	163 808.11
4	7	1	5	0	0	285 063.59	175 112.58
3	7	1	4	0	0	296 740.50	186 417.93
2	7	1	3	0	0	308 450.43	197 723.50
1	7	1	2	0	0	320 190.85	209 029.26
5	7	−1	5	0	0	343 421.85	231 346.86
4	7	−1	4	0	0	343 534.44	231 441.66
3	7	−1	3	0	0	343 624.95	231 518.06
2	7	−1	2	0	0	343 693.14	231 575.48
1	7	−1	1	0	0	343 738.62	231 613.89
1	7	1	0	0	0	355 588.70	242 929.78
2	7	1	1	0	0	367 442.41	254 221.87
3	7	1	2	0	0	379 321.81	265 508.07
4	7	1	3	0	0	391 226.26	276 787.72
5	7	1	4	0	0	403 153.14	
6	7	1	5	0	0	415 103.63	
1	0	0	0	1	0	10 477.401	
2	0	0	1	1	0	22 277.273	175 97.535
3	0	0	2	1	0	34 076.40	28 898.03
4	0	0	3	1	0		40 196.70
5	0	0	4	1	0	57 667.93	
4	2	0	4	1	0	211 736.36	
3	4	−1	4	1	0	172 613.71	
2	4	−1	3	1	0	184 558.70	
1	4	−1	2	1	0	196 457.05	
1	4	1	1	1	0		176 973.46
2	4	1	2	1	0	220 738.96	177 049.41
3	4	1	3	1	0	221 309.38	177 162.52
4	4	1	4	1	0	222 000.44	
5	4	1	5	1	0	222 785.48	
2	4	−1	1	1	0		199 445.46
3	4	−1	2	1	0	255 184.47	210 654.26
4	4	−1	3	1	0	266 770.73	221 831.24
5	4	−1	4	1	0	278 301.99	232 975.88
6	6	1	7	1	0	259 557.97	
4	6	1	5	1	0		165 578.79
3	6	1	4	1	0	294 447.99	
2	6	1	3	1	0	306 149.00	188 172.10
1	6	1	2	1	0	317 883.49	199 471.28
5	6	−1	5	1	0		221 818.90
4	6	−1	4	1	0	341 244.28	221 901.98
3	6	−1	3	1	0	341 325.90	221 969.20
2	6	−1	2	1	0	341 387.08	222 019.63
1	6	−1	1	1	0	341 427.90	222 053.55
1	6	1	0	1	0	353 276.22	233 368.15

Reuse of AIP Publishing content is subject to the terms: https://publishing.aip.org/authors/rights-and-permissions. Downloaded to IP: 144.82.108.120 On: Mon, 05 Sep 2016 21:20:40

TABLE I. (*Continued.*)

J'	V'[a]	K'[b]	J''	V''	K''	HDO–DOH	HDO–HOD
2	6	1	1	1	0		244 663.39
3	6	1	2	1	0	377 018.24	255 954.58
4	6	1	3	1	0	388 930.41	267 241.99
5	6	1	4	1	0	400 868.62	
2	3	0	1	2	0		27 199.93
3	3	0	2	2	0	36 029.20	38 483.79
5	3	0	4	2	0		61 039.19
4	5	−1	4	2	0		67 861.59
2	5	1	1	2	0		90 776.02
4	5	1	3	2	0	58 193.30	113 674.17
3	7	1	3	2	0		114 046.51
4	7	1	4	2	0		114 076.02
5	7	1	5	2	0		114 112.39
2	7	−1	1	2	0	153 087.88	
3	7	−1	2	2	0	165 116.07	
4	7	−1	3	2	0	177 216.64	159 070.44
5	7	−1	4	2	0	189 354.16	
3	2	0	2	3	0		29 241.95
4	2	0	3	3	0		40 528.55
2	6	−1	3	3	0	92 772.29	
1	6	1	1	3	0		104 827.74
2	6	1	2	3	0		104 846.19
3	6	−1	2	3	0	163 107.36	
4	6	−1	3	3	0	175 200.46	
5	6	−1	4	3	0	187 331.92	
4	3	0	3	4	1	38 651.31	
1	5	−1	1	4	1	992.18	3680.95
1	5	1	1	4	−1		3815.22
2	5	−1	2	4	1	472.69	3546.91
2	5	1	2	4	−1	2030.49	
3	5	−1	3	4	1	−254.42	3345.35
3	5	1	3	4	−1	2736.68	
4	5	1	4	4	−1	3613.63	4410.86
4	5	−1	4	4	1	−1153.96	3077.00
5	5	1	5	4	−1		4741.35
2	5	−1	1	4	−1		26 287.13
3	5	1	2	4	1	37 182.56	37 751.62
5	5	1	4	4	1	60 936.68	60 402.64
3	4	−1	2	5	−1	33 973.12	
5	4	1	4	5	1	58 549.83	
1	7	−1	1	6	1	939.60	4541.35
1	7	1	1	6	−1	1040.67	4572.55
2	7	−1	2	6	1	836.90	4509.23
2	7	1	2	6	−1	1139.94	4602.52
3	7	1	3	6	−1	1288.77	4645.16
3	7	−1	3	6	1	682.84	
4	7	1	4	6	−1	1487.05	
4	7	−1	4	6	1	477.65	
5	7	−1	5	6	1	221.24	
5	7	1	5	6	−1	1734.75	
3	7	−1	2	6	−1	36 314.40	
3	7	1	2	6	1	36 465.52	
5	7	−1	4	6	−1	59 845.22	
2	6	−1	1	7	−1	22 563.55	
3	6	1	2	7	1		29 333.22
3	6	−1	2	7	−1	34 339.90	
4	6	−1	3	7	−1		40 567.05
5	6	1	4	7	1	58 136.92	
5	6	−1	4	7	−1	57 884.02	

[a]V specifies the state number (0–7) of Fig. 2.

[b]The $K=+1$, -1, and 0 labels are used to denote the $J_{1,J-1}$, $J_{1,J}$, and $J_{0,J}$ levels, respectively, where the subscripts denote the limiting prolate and oblate quantum number labels.

are perturbed by the nearby $V=4$ and 5 levels through a strong b-type Coriolis interaction arising from the methylamine type tunneling motion. This Coriolis interaction allows the observation of two ''forbidden'' $K=0$ Q-branch lines, the $V=2\leftarrow1$, $4_{04}\leftarrow4_{04}$ and $V=3\leftarrow0$, $4_{04}\leftarrow4_{04}$ transitions. A further consequence of this perturbation is that the $V=5\leftarrow4$ asymmetry-tunneling transitions are poorly characterized by Eq. (1).

Reuse of AIP Publishing content is subject to the terms: https://publishing.aip.org/authors/rights-and-permissions. Downloaded to IP: 144.82.108.120 On: Mon, 05 Sep 2016 21:20:40

TABLE II. Spectroscopic constants for HDO–DOH and HDO–HOD (in MHz). The centrifugal distortion constants, D_V, are constrained to be the same for all the states of the same isotopomer.

	HDO–DOH	HDO–HOD
E_0	0.0	0.0
B_0	5899.8414(13)[a]	5650.3786(33)
D_0	0.046 08(12)	0.041 06(29)
E_1	1322.1019(43)	5004.059(20)
B_1	5899.0987(14)	5649.6818(94)
D_1	0.046 08(12)	0.041 06(29)
E_2	214 366.76(25)	117 630.47(24)
B_2	5908.27(47)	5644.838(15)
D_2	0.046 08(12)	0.041 06(29)
E_3	215 372.11(38)	122 255.52(24)
B_3	5908.59(46)	5644.378(18)
D_3	0.046 08(12)	0.041 06(29)
E_4	227 321.24(32)	187 591.22(16)
B_4	5896.33(23)	5651.809(13)
D_4	0.046 08(12)	0.041 06(29)
$(B-C)_4/4$	22.96(23)	16.7447(65)
E_5	228 585.28(30)	191 339.54(16)
B_5	5895.38(23)	5651.5660(99)
D_5	0.046 08(12)	0.041 06(29)
$(B-C)_5/4$	22.42(23)	16.5979(40)
E_6	348 671.535(96)	232 719.45(13)
B_6	5901.4763(53)	5645.021(13)
D_6	0.046 08(12)	0.041 06(29)
$(B-C)_6/4$	12.6249(30)	3.8187(64)
E_7	349 662.117(94)	237 277.30(12)
B_7	5901.0445(53)	5644.5989(88)
D_7	0.046 08(12)	0.041 06(29)
$(B-C)_7/4$	12.6072(27)	3.8422(51)
$\alpha_{3,5}$[b]	809.0(21)	
$\alpha_{2,4}$	809.0(21)	
σ[c]	0.29	0.34

[a]Experimental uncertainty is one standard deviation in units of the least significant digit.

[b]The Coriolis constants $\alpha_{3,5}$ and $\alpha_{2,4}$ are constrained to be equal in the least-squares fit.

[c]Standard deviation of the least-squares fit.

To model the Coriolis interaction we use an off-diagonal $\Delta K=\pm 1$ matrix element between states V and V' of the form,

$$\alpha_{V,V'}[J(J+1)]^{1/2}, \tag{3}$$

where $\alpha_{V,V'}$ is a constant to be determined in the fit. A similar Coriolis interaction is most likely present for HDO–HOD except the spectrum is less sensitive to this effect due to the larger energy separation between the $V=2$ and 3 levels and the $V=4$ and 5 levels for this isotopomer. The Coriolis interaction is diagonal in the donor–acceptor tunneling state, coupling the $J_{0,J}$ states for $V=2$ with the $J_{1,J-1}$ (i.e., $K=+1$ component in the notation of Table I for $V=4$ and the $J_{0,J}$ states for $V=3$ with the $J_{1,J-1}$ states for $V=5$. We note that $(H_2O)_2$, H_2O–DOH, and HDO–HOH all show the effects of strong Coriolis interactions between nearly degenerate $K=0$ and 1 states.

In Table II we show the spectroscopic constants for HDO–DOH and HDO–HOD resulting from the least squares fit of the frequencies of Table I to Eqs. (2) and (3). In the fit, the transitions were weighted by the reciprocal of the square of the measurement uncertainties, given at the bottom of Table I. For each isotopomer, the distortion constants were constrained to be the same for each of states 0 through 7. The standard deviations of the fits are 0.29 and 0.34 MHz for HDO–DOH and HDO–HOD, respectively. Constraining the Coriolis constants to zero in the fit for HDO–DOH gives a standard deviation of 35 MHz, an increase of more than 100 from the Coriolis fit.

DISCUSSION

In the present study we report the observation and analysis of the rotation-tunneling spectra of HDO–DOH and the higher energy HDO–HOD. Previous studies in seeded Ar beams of mixed deuterated-protonated water dimers revealed only the presence of the O–D bonded dimers. Moreover, an extensive study[45] of deuterated acetylene dimers using Ar as a carrier gas showed no evidence for H-bonded mixed H/D isotopomers. The present results indicate that the barriers between the H-bonded and D-bonded configurations are high enough and the zero-point binding energy differences small enough that the H-bonded species can be stabilized in He and mixed Ne/He expansions. Quantifying the energetics and the Ar, Ne, and He carrier gas dependence of the isotopomer formation dynamics is difficult due to our lack of knowledge of the H_2O dimer force field and the thermodynamics and kinetics of supersonic expansions.

Although the present results do not furnish much information on the energy separation between the H- and D-bonded dimers they do allow us to obtain some insight into the tunneling motions associated with the donor–acceptor interchange and the methyl-amine-type tunneling. The observed donor–acceptor tunneling splittings and selection rules provide information on the barriers and pathways for this tunneling process. For all three types of transitions, a, b, and c, in both isotopomers, the tunneling state selection rules are symmetric↔antisymmetric, indicating that the μ_a, μ_b, and μ_c electric dipole-moment components are antisymmetric functions of the tunneling coordinate. The HF dimerlike tunneling pathway, in which the two monomer OH or OD bonds interchange roles through a geared motion, satisfies these symmetry requirements on μ_a, μ_b, and μ_c.

It has been suggested[13] that an antigeared tunneling pathway is also contributing to the donor–acceptor tunneling splitting. In this picture, the tunneling splitting for states 0 and 1 is the sum and for 2 and 3 the difference of the tunneling splittings for the geared (ν_g) and antigeared (ν_a) pathways. Likewise, for $K=1$, states 6 and 7 are split by $\nu_g+\nu_a$ and states 4 and 5 are split by $\nu_g-\nu_a$. Previous application of this model to $(H_2O)_2$ and $(D_2O)_2$ gave $\nu_g \gg \nu_a$ and required that ν_g and ν_a change slightly with K.

If we consider antigeared tunneling pathways for HDO–DOH and HDO–HOD we obtain inconsistent results. Examination of Table III shows that for HDO–DOH the $V=7,6$ splitting is less than the $V=4,5$ splitting, whereas the $V=0,1$ splitting is greater than the $V=2,3$ splittings. If the antigeared tunneling pathway is important for HDO–DOH we would expect the $V=7,6$ splitting to be greater than the $V=4,5$ splitting. Unlike the case of HDO–DOH, the splittings shown in Table III for the HDO–HOD isotopomer have the correct energy ordering for the presence of both geared

Reuse of AIP Publishing content is subject to the terms: https://publishing.aip.org/authors/rights-and-permissions. Downloaded to IP: 144.82.108.120 On: Mon, 05 Sep 2016 21:20:40

TABLE III. Tunneling splittings for HDO–DOH and HDO–HOD (in MHz). Experimental uncertainty is one standard deviation in units of the least significant digit.

	HDO–DOH	HDO–HOD
Donor–acceptor tunneling splittings		
$V=0,1$	1322.1019(43)	5004.059(20)
$V=2,3$	1005.35 (45)	4625.05 (34)
$V=4,5$	1264.04 (44)	3748.32 (23)
$V=6,7$	990.58 (13)	4557.85 (18)
Methyl-amine-type tunneling splittings		
$K=0$	214 208.38 (23)	117 440.97 (17)
$K=1$	121 213.57 (71)	45533.00 (14)

and antigeared tunneling pathways. Our inability to interpret the observed tunneling splittings for both HDO–HOD and HDO–DOH using the presence of an antigeared tunneling pathway suggests an alternative mechanism for the variation of the donor–acceptor tunneling splitting between states with the same K. One possibility is that the donor–acceptor tunneling is coupled to the methyl-amine-like tunneling. This would make the donor-acceptor tunneling splitting a complex function of both K and methyl-amine-like tunneling state.

To model the donor–acceptor tunneling splittings in HDO–DOH and HDO–HOD requires knowledge of the tunneling potential and reduced mass for tunneling. The double-minima donor–acceptor tunneling potentials for HDO–DOH and HDO–HOD can be pictured as resulting from deformation of the four-equivalent-minima donor–acceptor tunneling potentials of $(H_2O)_2$ or $(D_2O)_2$,[25] as shown qualitatively in Fig. 3. In both $(H_2O)_2$ and $(D_2O)_2$ the donor–acceptor tunneling splittings were approximately modeled[25] by picturing the tunneling motions as resulting from a geared internal rotation of the two water units about their C_2 symmetry axis using the Hamiltonian,

$$H=F\mathbf{p}^2+\frac{V_4}{2}(1-\cos 4\alpha), \tag{4}$$

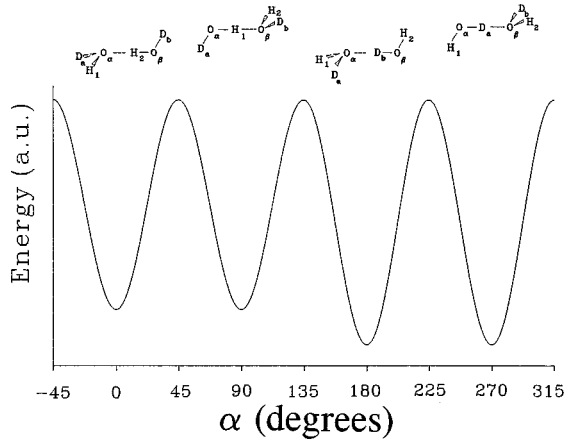

FIG. 3. Qualitative picture of a one dimensional donor–acceptor interchange tunneling potential for the two isotopomers of $(HOD)_2$.

where $F=b_0/2$, and b_0 is the zero-point rotational constant of H_2O or D_2O about the C_2 symmetry axis (i.e., b inertial axis). $F=3.635$ cm^{-1} for $(D_2O)_2$ and 7.260 cm^{-1} for $(H_2O)_2$. The Hamiltonian matrix is set up in the free-rotor basis $|m\rangle=e^{im\alpha}/(2\pi)^{1/2}$ and diagonalized to obtain eigenvalues. Using the above values for F and fitting the tunneling splitting associated with the $A_1^{\pm}/B_1^{\pm}$ states [1172.115(14) MHz (Ref. 15) for $(D_2O)_2$ and 22 554.37(30) MHz (Ref. 14) for $(H_2O)_2$], gives $V_4=402$ cm^{-1} and 437 cm^{-1} for $(D_2O)_2$ and $(H_2O)_2$, respectively.

For the pseudo-double-minima potentials of $(DOH)_2$ we use a potential consisting of two of the minima of the four-fold potential of Eq. (4) by approximating $V(\alpha)$ for $\alpha\in[-\pi/4, 7\pi/4]$ by

$$V(\alpha)=V_4(1-\cos 4\alpha)/2 \quad \text{for } \alpha\in[-\pi/4,3\pi/4] \tag{5}$$

and

$$V(\alpha)=V_4 \quad \text{for } \alpha\in[3\pi/4,7\pi/4]. \tag{6}$$

Model calculations indicate that placing two minima (centered at $\alpha=\pi$ and $\alpha=3\pi/2$) corresponding to the other isotopomer for $\alpha\in[3\pi/4,7\pi/4]$ does not affect appreciably the calculated tunneling splittings. The effect is only 2 MHz out of ~4500 MHz when we include two additional minima of the form $V_4(1-\cos 4\alpha)/2+\Delta$ with $V_4=399$ cm^{-1} and $\Delta=1$ cm^{-1}, when the initial minima have $V_4=400$ cm^{-1}.

As a first approximation for the reduced mass for tunneling for HDO–DOH and HDO–HOD we use $F=5.4475$ cm^{-1}, which is the average of the F values for the totally deuterated and protonated dimers. With this F value we calculate tunneling splittings of 4341 and 3222 MHz for $V_4=402$ and 437 cm^{-1}, respectively. The observed tunneling splittings for HDO–DOH and HDO–HOD are 1322 and 5004 MHz. Since the calculated tunneling splittings scale with F value, these results suggest that the F value for HDO–DOH is smaller and that of HDO–HOD is larger than the average of the deuterated and protonated values.

If we assume that the barriers for HDO–DOH and HDO–HOD lie between 402 and 437 cm^{-1} we find that F values from 4.24–4.54 cm^{-1} for HDO–DOH and from 5.62–6.00 cm^{-1} for HDO–HOD reproduce the experimental tunneling splittings. The larger F value for HDO–HOD compared to HDO–DOH indicates that in HDO–HOD the reduced mass is dominated more by movement of the proton and in HDO–DOH it is dominated more by movement of the deuteron. This difference in F values seems reasonable since pictorially the atom involved in the hydrogen bonding has to move the most in the tunneling. As an aside, we note that the effective F value for HDO–DOH is nearly equal to $b_0/2=4.55$ cm^{-1} for HDO, suggesting that in HDO–DOH the tunneling process may be viewed as a geared internal rotation of the two HDO moieties about their b inertial axes.

In addition to the donor–acceptor tunneling splitting, we have also measured splittings arising from the methyl-amine-type tunneling motion corresponding to the inversion of the configuration of the HDO–H or HDO–D part of the molecule through a planar or near-planar transition state and the internal rotation of the off-axis H or D of the proton donor by 180° about the O–HO or O–DO axis. In HDO–HOD these

Reuse of AIP Publishing content is subject to the terms: https://publishing.aip.org/authors/rights-and-permissions. Downloaded to IP: 144.82.108.120 On: Mon, 05 Sep 2016 21:20:40

splittings are remarkably close to those observed in HDO–DOD giving clear evidence that the H or D associated with the hydrogen bond plays only a small role in the high frequency tunneling process. In HDO–HOD the $K=1$ methylamine-type splitting is 45 533.00(14) MHz while the equivalent splitting in HDO–DOD is 42 994.08(4) MHz.[24] Similarly, for $K=0$, the HDO–HOD splitting is 117 440.97(17) MHz while in HDO–DOD the splitting is 107 723.64(14) MHz.[33] Moreover, since the inner H/D is nearly on the center of mass of the dimer the A, B, and C rotational constants are not affected strongly by isotopic substitution of the proton-donating D/H. Thus, in addition to supporting the proposed tunneling pathway, the small isotopic shifts simplify the assignment of the isotopic spectra, since knowing the $\Delta K=1$ bands positions for an O–H or O–D bonded species leads to relatively good predictions for the positions of the $\Delta K=1$ bands for the isotopomer differing by isotopic substitution of the H or D doing the proton donation.

A quantitative model has not yet been developed to calculate the tunneling splittings associated with the methylamine-type tunneling. Since this tunneling motion is strongly coupled to the K or a-axis rotation it will be necessary, at the minimum, to include this rotational degree of freedom. More extensive isotopic studies recently undertaken[33] will furnish a critical test for any model developed to interpret these tunneling splittings.

Future efforts will need to be devoted to calculating multiple tunneling splittings from suitable model potential energy surfaces. Indeed, some effort has been extended in this area for modeling the proton tunneling in malonaldehyde.[46] Large scale variational calculations, such as those recently undertaken on the ammonia dimer,[47] which use free-rotor expansions of the vibrational-tunneling wave functions, have just recently become possible for the more anisotropic water dimer system.[48] Ideally, any method developed to model the tunneling splittings in the water dimer must be both accurate and efficient enough to allow the large body of spectroscopic data available on the water dimer to be used in the refinement of the water pair potential.

ACKNOWLEDGMENTS

We would like to thank NATO (Grant No. 921-278), the Russian Fund for Fundamental Studies, and the International Science Foundation (Registration No. Ph3-1137) for partial support of this work.

[1] For a review see, G. T. Fraser, Inter. Rev. Phys. Chem. **10**, 189 (1991).
[2] T. R. Dyke and J. S. Muenter, J. Chem. Phys. **60**, 2929 (1974).
[3] T. R. Dyke, J. Chem. Phys. **66**, 492 (1977).
[4] T. R. Dyke, K. M. Mack, and J. S. Muenter, J. Chem. Phys. **66**, 498 (1977).
[5] J. A. Odutola and T. R. Dyke, J. Chem. Phys. **72**, 5062 (1980).
[6] J. T. Hougen, J. Mol. Spectrosc. **114**, 395 (1985).
[7] L. H. Coudert, F. J. Lovas, R. D. Suenram, and J. T. Hougen, J. Chem. Phys. **87**, 6290 (1987).
[8] T. R. Dyke, in *Structure and Dynamics of Weakly Bound Molecular Complexes*, edited by A. Weber (Reidel, Boston, 1987), p 43.
[9] D. D. Nelson, Jr. and W. Klemperer, J. Chem. Phys. **87**, 139 (1987).
[10] J. A. Odutola, T. A. Hu, D. Prinslow, S. E. O'Dell, and T. R. Dyke, J. Chem. Phys. **88**, 5352 (1988).
[11] L. Martinache, S. Jans-Bürli, B. Vogelsanger, W. Kresa, and A. Bauder, Chem. Phys. Lett. **149**, 424 (1988).
[12] Z. S. Huang and R. E. Miller, J. Chem. Phys. **88**, 8008 (1988).
[13] L. H. Coudert and J. T. Hougen, J. Mol. Spectrosc. **130**, 86 (1988).
[14] G. T. Fraser, R. D. Suenram, and L. H. Coudert, J. Chem. Phys. **90**, 6077 (1989).
[15] R. D. Suenram, G. T. Fraser, F. J. Lovas, J. Mol. Spectrosc. **138**, 440 (1989). There are a couple of typographical errors in Table I. The transitions at 663 13.13, 640 00.45, and 748 52.29 MHz should be labeled as $B_1^{\pm}6_{06}-5_{05}$, $A_1^{\pm}6_{06}-5_{05}$, and $B_1^{\pm}7_{07}-6_{06}$, respectively.
[16] T. A. Hu and T. R. Dyke, J. Chem. Phys. **91**, 7348 (1989).
[17] G. T. Fraser, R. D. Suenram, L. H. Coudert, and R. S. Frye, J. Mol. Spectrosc. **137**, 244 (1989).
[18] Z. S. Huang and R. E. Miller, J. Chem. Phys. **91**, 6613 (1989).
[19] K. L. Busarow, R. C. Cohen, G. A. Blake, K. B. Laughlin, Y. T. Lee, and R. J. Saykally, J. Chem. Phys. **90**, 3937 (1989).
[20] L. H. Coudert and J. T. Hougen, J. Mol. Spectrosc. **139**, 259 (1990).
[21] E. Zwart, J. J. ter Meulen, and W. L. Meerts, Chem. Phys. Lett. **166**, 500 (1990).
[22] E. Zwart, J. J. ter Meulen, and W. L. Meerts, Chem. Phys. Lett. **173**, 115 (1990).
[23] N. Pugliano and R. J. Saykally, J. Chem. Phys. **96**, 1832 (1992).
[24] E. N. Karyakin, G. T. Fraser, B. Pate, and R. D. Suenram, J. Mol. Spectrosc. **161**, 312 (1993).
[25] E. N. Karyakin, G. T. Fraser, R. D. Suenram, Mol. Phys. **78**, 1179 (1993).
[26] N. Pugliano, J. D. Cruzan, J. G. Loeser, and R. J. Saykally, J. Chem. Phys. **98**, 6600 (1993).
[27] W. Stahl and L. H. Coudert, J. Mol. Spectrosc. **157**, 161 (1993).
[28] See, for example, S. S. Xantheas and T. H. Dunning, Jr., J. Chem. Phys. **98**, 8037 (1993); D. Feller, *ibid*. **96**, 6104 (1992), and references therein.
[29] B. J. Smith, D. J. Swanton, J. A. Pople, H. F. Schaefer III, and L. Radom, J. Chem. Phys. **92**, 1240 (1990).
[30] See, for example, W. L. Jorgensen, J. Chandrasekhar, J. D. Madura, R. W. Impey, and M. L. Klein, J. Chem. Phys. **79**, 926 (1983); M. J. Wójcik and S. A. Rice, *ibid*. **84**, 3042 (1986), and references therein.
[31] J. Z. Gillies, C. W. Gillies, R. D. Suenram, F. J. Lovas, T. Schmidt, and D. Cremer, J. Mol. Spectrosc. **146**, 493 (1991). There is a typographical error in the footnote giving the frequencies of the four observed HDO–DOH lines. The 21 915.533 MHz line should be 24 915.533 MHz.
[32] The splitting between the symmetric and antisymmetric tunneling states in $(D_2O)_2$ and $(H_2O)_2$ have been divided by 2 in making this comparison since in the homogenous dimers the donor–acceptor interchange potential has four minima.
[33] E. N. Karyakin, G. T. Fraser, R. D. Suenram, and F. J. Lovas (unpublished).
[34] G. T. Fraser, A. S. Pine, W. J. Lafferty, and R. E. Miller, J. Chem. Phys. **87**, 1502 (1987).
[35] G. T. Fraser and A. S. Pine, **91**, 637 (1989).
[36] T. E. Gough, R. E. Miller, and G. Scoles, Appl. Phys. Lett. **30**, 338 (1977).
[37] Yu. I. Alekshin, G. M. Altshuller, O. P. Pavlovsky, E. N. Karyakin, A. F. Krupnov, D. G. Paveliev, and A. P. Shkaev, Int. J. Infra. Millimeter Waves **11**, 961 (1990).
[38] G. T. Fraser, A. S. Pine, J. L. Domenech, and B. H. Pate, J. Chem. Phys. **99**, 2396 (1993).
[39] T. J. Balle and W. H. Flygare, Rev. Sci. Instrum. **52**, 33 (1981).
[40] F. J. Lovas and R. D. Suenram, J. Chem. Phys. **87**, 2010 (1987).
[41] R. D. Suenram, F. J. Lovas, G. T. Fraser, J. Z. Gillies, C. W. Gillies, and M. Onda, J. Mol. Spectrosc. **137**, 127 (1989).
[42] F. J. Lovas, N. Zobov, W. J. Stevens, G. T. Fraser, and R. D. Suenram, J. Mol. Spectrosc. (submitted).
[43] J.-U. Grabow and W. Stahl, Z. Naturforsh. **A45**, 1043 (1990).
[44] T. D. Klots, R. S. Ruoff, and H. S. Gutowsky, J. Chem. Phys. **90**, 4216 (1989).
[45] K. Matsumura, F. J. Lovas, and R. D. Suenram, J. Mol. Spectrosc. **150**, 576 (1991).
[46] T. Carrington, Jr. and W. H. Miller, J. Chem. Phys. **84**, 4364 (1986).
[47] J. W. I. van Bladel, A. van der Avoird, P. E. S. Wormer, and R. J. Saykally, J. Chem. Phys. **97**, 4750 (1992).
[48] S. C. Althorpe and D. C. Clary, J. Chem. Phys. **101**, 3603 (1994).

Reuse of AIP Publishing content is subject to the terms: https://publishing.aip.org/authors/rights-and-permissions. Downloaded to IP: 144.82.108.120 On: Mon, 05 Sep 2016 21:20:40